Electronic Supporting Information

Multiphase transition of supramolecular metallogels triggered by temperature

Bo Jiang, Li-Jun Chen, Guang-Qiang Yin, Yu-Xuan Wang,*
*Wei Zheng, Lin Xu and Hai-Bo Yang**

Shanghai Key Laboratory of Green Chemistry and Chemical Processes,
School of Chemistry and Molecular Engineering, East China Normal
University, Shanghai 200062, P. R. China.

E-mail: hbyang@chem.ecnu.edu.cn
15121162876@163.com

Table of Contents

1. General Information

All solvents were dried according to standard procedures and all of them were degassed under N_2 for 30 minutes before use. All air-sensitive reactions were carried out under inert N_2 atmosphere. ^{1}H and ^{31}P NMR spectra were recorded on Bruker 400 MHz Spectrometer (^{1}H: 400 MHz; ^{31}P: 161.9 MHz) at 298 K. The ^{1}H and ^{13}C NMR chemical shifts are reported relative to the residual solvent signals, and ^{31}P NMR resonances are referenced to an internal standard sample of 85% H_3PO_4 (δ 0.0). Coupling constants (J) are denoted in Hz and chemical shifts (δ) in ppm. Multiplicities are denoted as follows: s = singlet, d = doublet, m = multiplet, br = broad. IR spectra were recorded on a Bruker Tensor 27 infrared spectrophotometer. The CSI-TOF-MS spectra were acquired by using an AccuTOF CS mass spectrometer (JMS-T100CS, JEOL, Tokyo, Japan). UV−vis spectra were recorded in a quartz cell (light path 10 mm or 2 mm) on a Cary 50Bio UV-visible spectrophotometer. Steady-state fluorescence spectra were recorded in a conventional quartz cell (light path 10 mm or 2 mm) on a Cary Eclipse fluorescence spectrophotometer. SEM images were obtained by using a S-4800 (Hitachi Ltd.) with an accelerating voltage of 3.0-10.0 kV. Samples were prepared by dropping dilute gels or solutions onto a silicon wafer. To minimize the charge of samples, a thin layer of Au was deposited onto the samples before SEM examination.

2. Synthetic Experimental Details and Characterizations of New Compounds

The hydrophilic oligoether dendrons **1** and chloroplatinum(II) precursors **8** were prepared according to reported procedures.[1-2]

Scheme S1. Synthesis route of hydrophilic oligo(ethylene oxide) dendritic chains **6**.

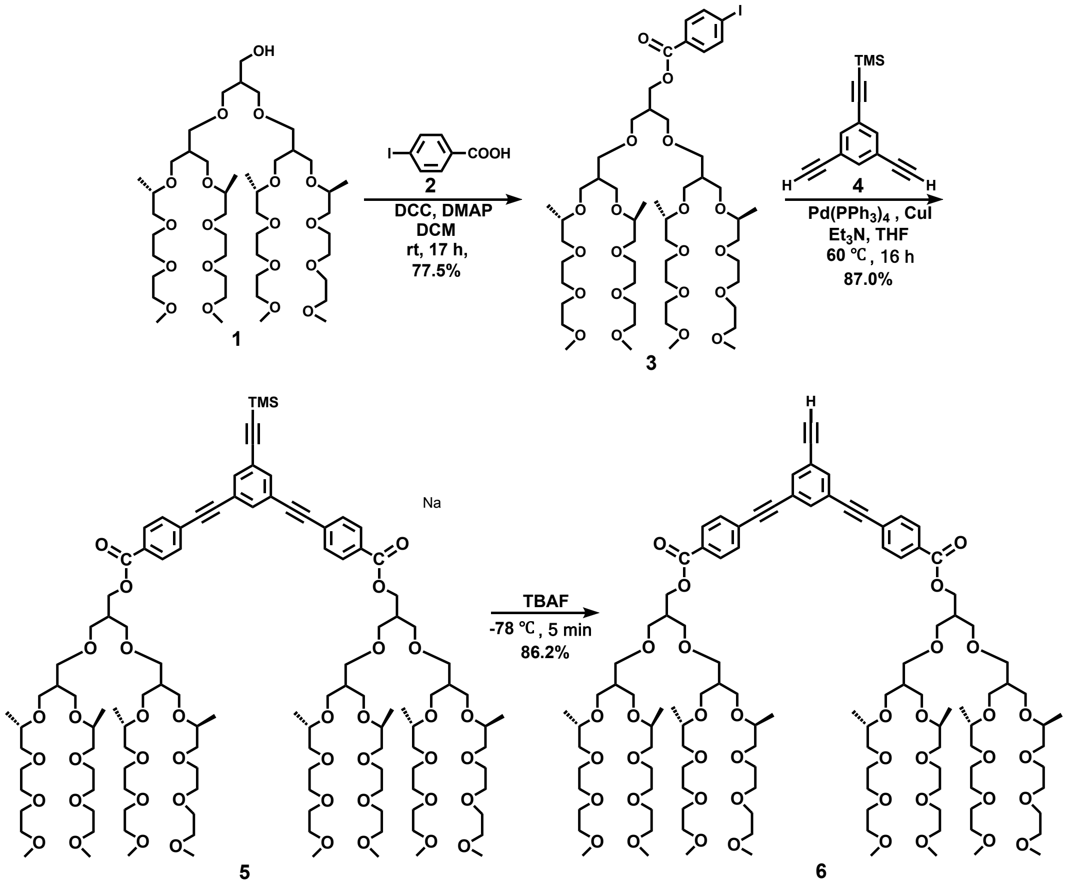

Synthesis of compound 3. A 50 mL Schlenk flask was charged with **1** (450 mg, 0.49 mmol), **2** (180 mg, 0.73 mmol), DMAP (25 mg, 0.2 mmol) and DCC (262 mg, 1.27 mmol), degassed, and back-filled three times with N_2. Anhydrous dichloromethane (8 mL) were introduced into the reaction flask by syringe. The mixture was stirred under an inert atmosphere at 0 °C for 5 min and at room temperature for 17 h. After filtration, the solvent was removed by evaporation on a rotary evaporator. The residue was purified by column chromatography on silica gel (ethyl acetate/methanol = 20:1) to give **3** (436 mg, 77.5%) as a colorless liquid. R$_f$ = 0.68 (ethyl acetate/methanol = 20:1). ^{1}H NMR (400 MHz; CDCl$_3$): δ 7.81 (d, *J* = 8.4 Hz, 2H), 7.73 (d, *J* = 8.4 Hz, 2H), 4.37 (d, *J* = 5.7 Hz, 2H), 3.37-3.65 (m, 72H), 2.31-2.37 (m, 1H), 2.03-2.08 (m, 2H), 1.10 (d, *J* = 6.1 Hz, 12H); ^{13}C NMR (CDCl$_3$; 100 MHz): δ 165.82, 137.65, 130.92, 129.74, 100.55, 74.93, 74.70, 74.68, 71.86, 70.66, 70.54, 70.44, 69.54, 69.14, 67.27, 63.67, 58.94, 40.69, 39.39, 17.02. MALDI-TOF-MS of **3**: m/z calcd for $C_{51}H_{93}INaO_{20}$ ([M+Na]$^+$): 1175.52, found: 1174.89.

Synthesis of compound 5. A 50 mL Schlenk flask was charged with **3** (400 mg, 0.35 mmol), **4** (36 mg, 0.16 mmol), tetrakis(triphenylphosphine)palladium(II) (37.0 mg, 20 mol%), and cuprous iodide (6 mg, 20 mol%), degassed, and back-filled three times with N$_2$. Triethylamine (2.0 mL) and dried THF (2.0 mL) were introduced into the reaction flask by syringe. The reaction was stirred under an inert atmosphere at 60 °C for 16 h. The solvent was removed by evaporation on a rotary evaporator. The residue was purified by column chromatography on silica gel (ethyl acetate/methanol = 10:1) to give **5** (320 mg, 87.0%) as a colorless liquid. R$_f$ = 0.70 (ethyl acetate/methanol = 10:1). ^{1}H NMR (400 MHz; CDCl$_3$): δ 8.02 (d, *J* = 8.4 Hz, 4H), 7.66 (s, 1H), 7.64 (s, 2H), 7.58 (d, *J* = 8.4 Hz, 4H), 4.39 (d, *J* = 5.7 Hz, 4H), 3.37-3.65 (m, 144H), 2.35-2.38 (m, 2H), 2.06-2.10 (m, 4H), 1.11 (d, *J* = 6.1 Hz, 24H), 0.26 (s, 9H); ^{13}C NMR (CDCl$_3$; 100 MHz): δ 165.68, 134.86, 134.23, 131.53, 129.99, 129.47, 127.24, 124.07, 123.40, 102.81, 96.17, 90.33, 89.71, 74.93, 74.71, 74.69, 71.87, 70.67, 70.55, 70.47, 69.53, 69.14, 67.30, 63.63, 58.97, 40.71, 39.42, 17.05. MALDI-TOF-MS of **5**: m/z calcd for $C_{117}H_{198}NaO_{40}Si$ ([M+Na]$^+$): 2294.31, found: 2292.32.

Synthesis of compound 6. To a stirred solution of **5** (150 mg, 0.07 mmol) in THF (10 mL), tetrabutylammonium fluoride (0.1 mL, 1.0 M in THF, 0.1 mmol) was added dropwise at -78 ℃. The mixture was stirred for 5 min at -78 ℃. The solvent was removed by evaporation on a rotary evaporator. The residue was purified by column chromatography on silica gel (ethyl acetate/methanol = 20:1) to give **6** (125 mg, 86.2%) as a colorless liquid. $R_f = 0.70$ (ethyl acetate/methanol = 10:1). ^{1}H NMR (400 MHz; $CDCl_3$): δ 8.03 (d, *J* = 8.2 Hz, 4H), 7.70 (s, 1H), 7.64 (s, 2H), 7.59 (d, *J* = 8.1 Hz, 4H), 4.39 (d, *J* = 5.6 Hz, 4H), 3.37-3.65 (m, 144H), 3.14 (s, 1H), 2.34-2.37 (m, 2H), 2.04-2.10 (m, 4H), 1.11 (d, *J* = 6.0 Hz, 24H); ^{13}C NMR ($CDCl_3$; 100 MHz): δ 165.66, 134.96, 134.65, 131.54, 130.03, 129.46, 127.13, 123.54, 123.06, 90.13, 89.87, 81.59, 78.75, 74.91, 74.69, 74.67, 71.84, 70.65, 70.53, 70.44, 69.51, 69.12, 67.27, 63.62, 58.95, 40.68, 39.39, 17.02. MALDI-TOF-MS of **6**: m/z calcd for $C_{114}H_{190}NaO_{40}$ ($[M+Na]^+$): 2222.27, found: 2220.38.

Scheme S2. Synthesis route of the Y-shaped amphiphilic alkynylplatinum(II) bzimpy complex **Y1**.

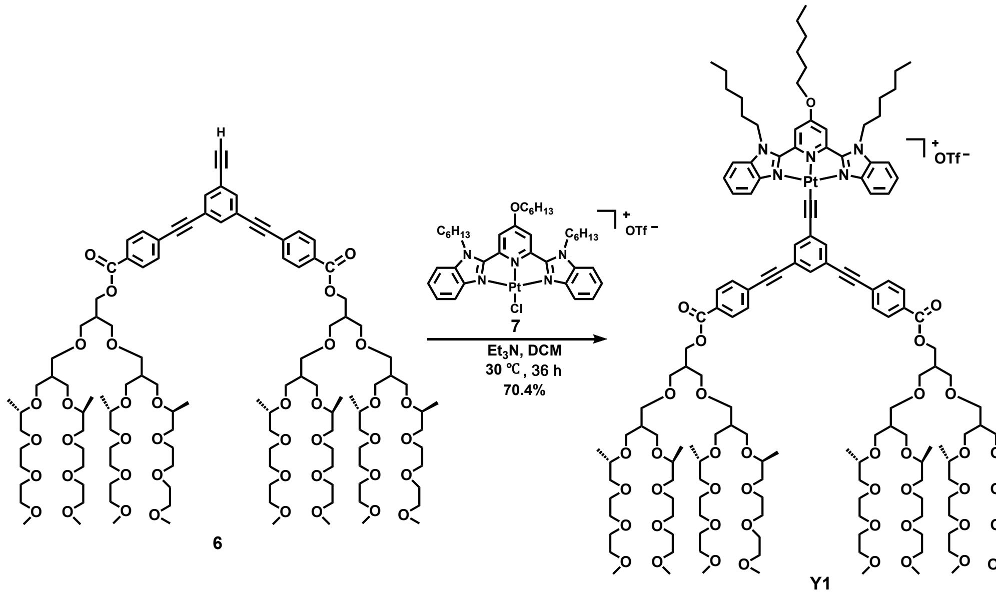

Synthesis of compound 7. The procedure was similar to that used to prepare **8**, except that 2, 6-bis(1-hexylbenzimidazol-2’-yl)-pyridine (2.0 g, 3.45 mmol) was used in place of 2,6-bis(1-dodecylbenzimi-dazol-2’-yl)-pyridine and the product was isolated as a trifluoromethane-sulfonate salt (2.4 g, 72.5%). $R_f = 0.61$ (DCM/acetone = 5:1). ^{1}H NMR (400 MHz; $CDCl_3$): δ 7.61 (d, *J* = 8.3 Hz, 2H), 7.29 (s, 1H), 7.19-7.23 (m, 2H), 7.15 (s, 2H), 7.01-7.05 (m, 2H), 4.46 (t, *J* = 6.4 Hz, 2H), 4.40 (t, *J* = 6.8 Hz, 4H), 1.97-2.04 (m, 2H), 1.73-1.81 (m, 4H), 1.45-1.48 (m, 4H), 1.25-1.30 (m, 11H), 0.98-1.02 (m, 3H), 0.86-0.89 (m, 9H); ^{13}C NMR ($CDCl_3$; 100 MHz): δ 169.43, 151.76, 148.30, 138.92, 134.09, 126.36, 126.28, 122.30, 119.75, 117.12, 111.75, 109.55, 71.62, 45.77, 31.56, 31.33, 30.06, 28.63, 26.16, 25.46, 22.58, 22.40, 14.03, 13.89. MALDI-TOF-MS of **7**: m/z calcd for $C_{37}H_{49}ClN_5OPt$ ($[M\text{-}OTf]^+$): 809.33, found: 810.16.

Synthesis of compound Y1. To a degassed solution of the chloroplatinum(II) precursor **7** (87 mg, 0.09 mmol) in CH_2Cl_2 (15 mL) were added compound **6** (100 mg, 0.05 mmol), a catalytic amount of CuI (2 mg, 10%), and NEt_3 (2 mL). The resultant solution was stirred at 30 ℃ for 36 h under an inert atmosphere. The solvent was removed by evaporation on a rotary evaporator. The residue was purified by column chromatography on silica gel (DCM/acetone = 1:1) to give **Y1** (100 mg, 70.4%) as a red viscous solid. $R_f = 0.79$ (DCM/acetone = 1:1). IR (neat): ν/cm^{-1} 2867, 2114, 1721, 1606, 1573, 1484, 1463, 1452, 1372, 1352, 1306, 1270, 1100, 1030, 1017, 932, 852, 769, 751, 696. ^{1}H NMR (400 MHz; $CDCl_3$): δ 8.53-8.55 (m, 2H), 8.06 (d, *J* = 8.3 Hz, 4H), 7.73 (s, 1H), 7.70 (s, 2H), 7.63-7.66 (m, 8H), 7.53 (s, 2H), 7.44-7.46 (m, 2H), 4.77 (s, 4H), 4.46 (t, *J* = 5.8 Hz, 2H), 4.40 (d, *J* = 5.7 Hz, 4H), 3.37-3.63 (m, 144H), 2.34-2.40 (m, 2H), 2.05-2.11 (m, 4H), 1.86-1.95 (m, 6H), 1.25-1.43 (m, 22H), 1.12 (d, *J* = 6.2 Hz, 24H), 0.82-0.89 (m, 9H); ^{13}C NMR ($CDCl_3$; 100 MHz): δ 169.99, 165.72, 152.28, 147.81, 139.45, 134.36, 134.19, 131.67, 130.18, 129.59, 127.65, 127.43, 127.22, 123.86, 118.78, 111.78, 110.07, 90.67, 90.01, 74.96, 74.76, 74.71, 71.90, 70.70, 70.56, 70.47, 69.62, 69.16, 67.37, 67.35, 63.72, 58.97, 46.55, 40.76, 39.51, 31.48, 31.19, 30.13, 28.55, 26.36, 25.36, 22.47, 22.35, 17.06, 13.98, 13.84. MALDI-TOF-MS of **Y1**: m/z calcd for $C_{151}H_{238}N_5O_{41}Pt$ ($[M\text{-}OTf]^+$): 2972.63, found: 2974.09.

Scheme S3. Synthesis route of the Y-shaped amphiphilic alkynylplatinum(II) bzimpy complex **Y2**.

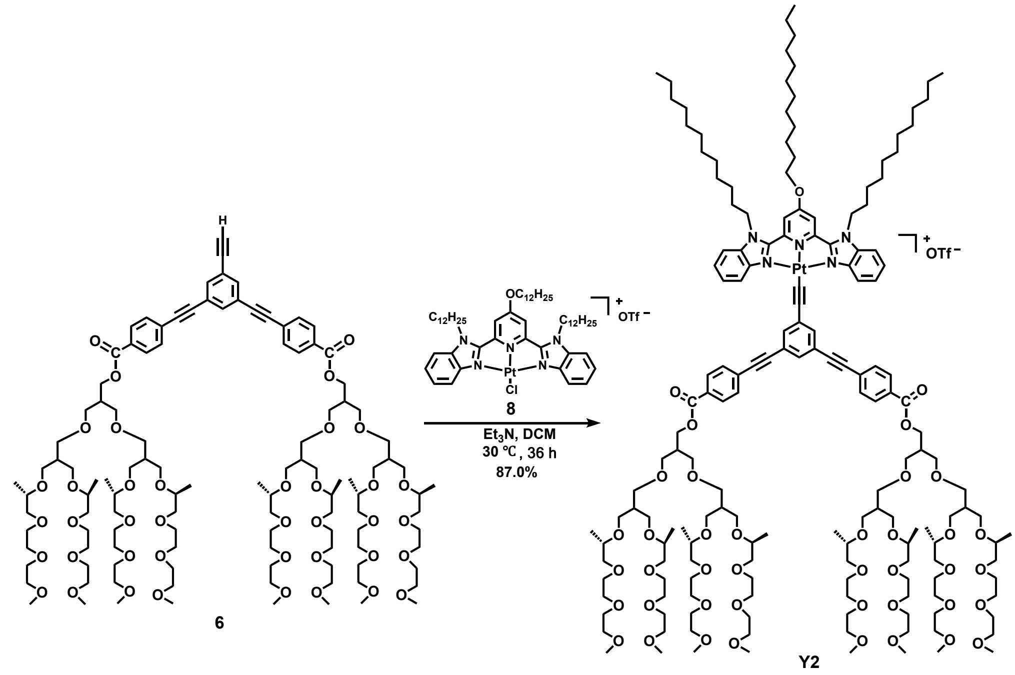

Synthesis of compound Y2. Following the procedure for the preparation of **Y1**. **6** (225 mg, 0.10 mmol), **8** (218 mg, 0.18 mmol), cuprous iodide (4 mg, 20 mol %), Et_3N (2 mL) and dried DCM (35 mL) yielded **Y2** as a red viscous solid (300 mg, 87.0%) after purification by column chromatography on silica gel (DCM/acetone = 1:1). R_f = 0.64 (DCM/acetone = 1:1). IR (neat): ν/cm^{-1} 2923, 2855, 2111, 1722, 1606, 1573, 1484, 1467, 1452, 1372, 1269, 1102, 1030, 1017, 854, 768, 753. ^1H NMR (400 MHz; $CDCl_3$): δ 8.58 (s, 2H), 8.06 (d, *J* = 8.2 Hz, 4H), 7.72 (s, 3H), 7.66 (d, *J* = 8.0 Hz, 8H), 7.57 (s, 2H), 7.45 (s, 2H), 4.79 (s, 4H), 4.78 (s, 2H), 4.39 (s, 4H), 3.37-3.65 (m, 144H), 2.36-2.37 (m, 2H), 2.07-2.09 (m, 4H), 1.93 (m, 6H), 1.19-1.23 (m, 54H), 1.11 (d, *J* = 6.2 Hz, 24H), 0.83-0.88 (m, 9H); ^{13}C NMR ($CDCl_3$; 100 MHz): δ 170.09, 165.70, 152.28, 147.80, 139.48, 134.40, 134.24, 133.14, 131.65, 130.17, 129.58, 127.67, 127.53, 127.40, 127.25, 123.82, 122.05, 119.50, 118.90, 111.71, 110.11, 90.71, 89.95, 74.96, 74.76, 74.72, 71.89, 70.69, 70.56, 70.45, 69.62, 69.16, 67.34, 67.32, 63.73, 58.95, 46.29, 40.76, 39.52, 31.81, 30.16, 29.67, 29.65, 29.62, 29.54, 29.50, 29.42, 29.32, 29.24, 29.14, 28.63, 26.69, 25.73, 22.59, 17.04, 14.07, 14.04. MALDI-TOF-MS of **Y2**: m/z calcd for $C_{169}H_{274}N_5O_{41}Pt$ ($[M-OTf]^+$): 3224.92, found: 3226.85.

Reference:

[1] H.-J. Kim, W.-C. Zin, M. Lee, *J. Am. Chem. Soc.* **2004**, *126*, 7009-7014.

[2] A. Y.-Y. Tam, W. H. Lam, K. M.-C. Wong, N. Zhu, V. W.-W. Yam, *Chem. Eur. J.* **2008**, *14*, 4562-4576.

3. UV-vis Absorption Spectra and Fluorescence Spectra

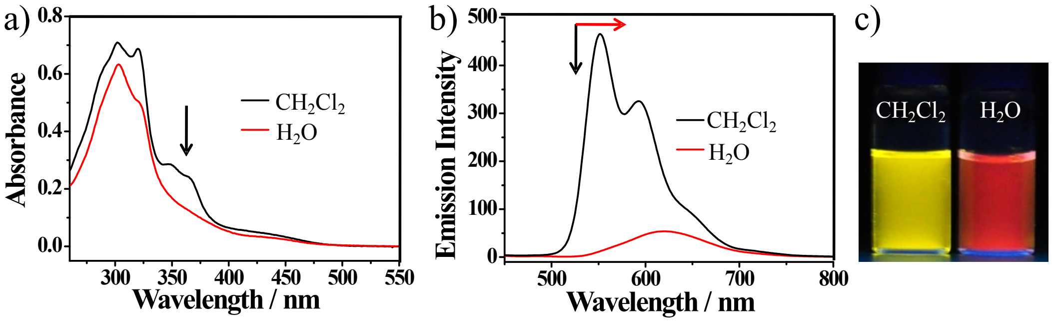

Figure S1. a) UV-vis absorption spectra and b) emission spectra of **Y1** (3.2×10^{-5} M) in different solvents at room temperature. c) The photograph shows the corresponding emission color changes upon changing the solvent composition.

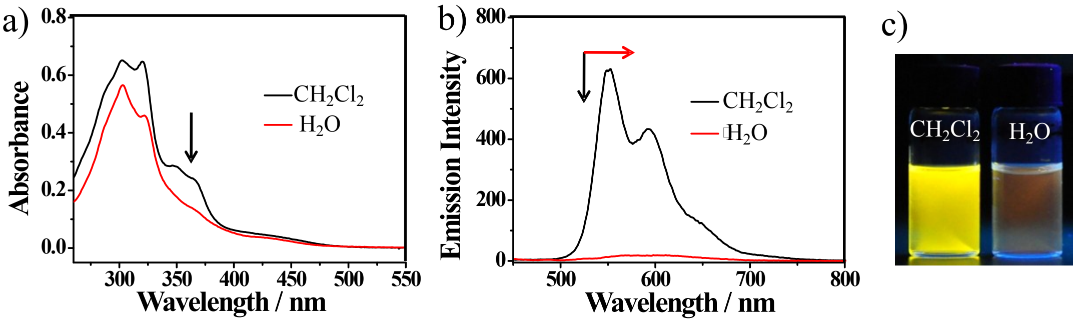

Figure S2. a) UV-vis absorption spectra and b) emission spectra of **Y2** (3.0×10^{-5} M) in different solvents at room temperature. c) The photograph shows the corresponding emission color changes upon changing the solvent composition.

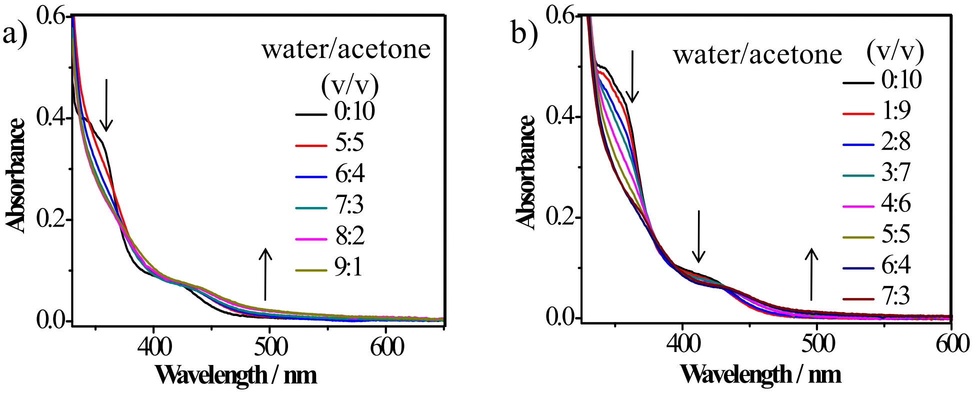

Figure S3. UV-vis absorption spectra of a) **Y1** (10^{-5} M) and b) **Y2** (10^{-5} M) upon increasing the water content in acetone at room temperature.

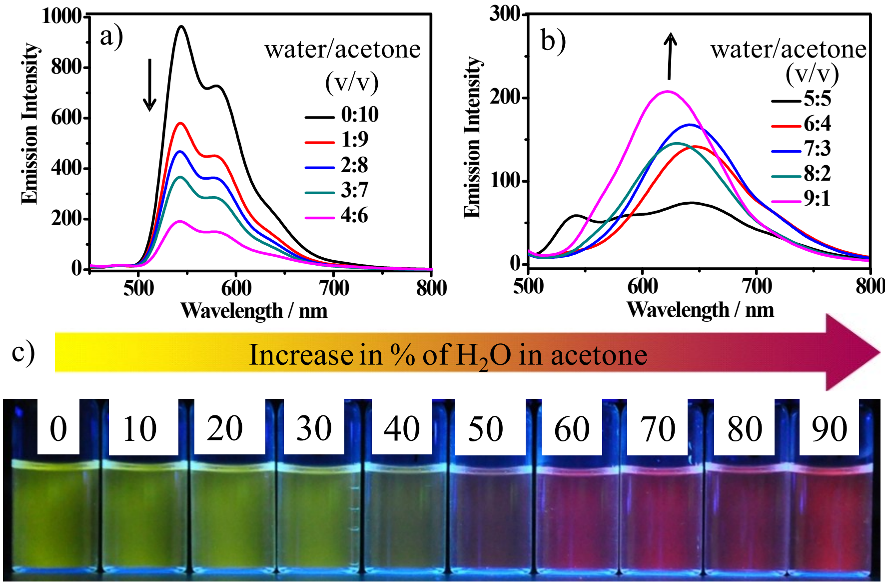

Figure S4. Emission spectra (λ_{ex} = 420 nm) of **Y1** (10^{-5} M) upon increasing the water content in acetone a) from 0 to 40% and b) from 50 to 90%. c) Photographs of **Y1** in water/acetone mixtures under a 365 nm UV lamp.

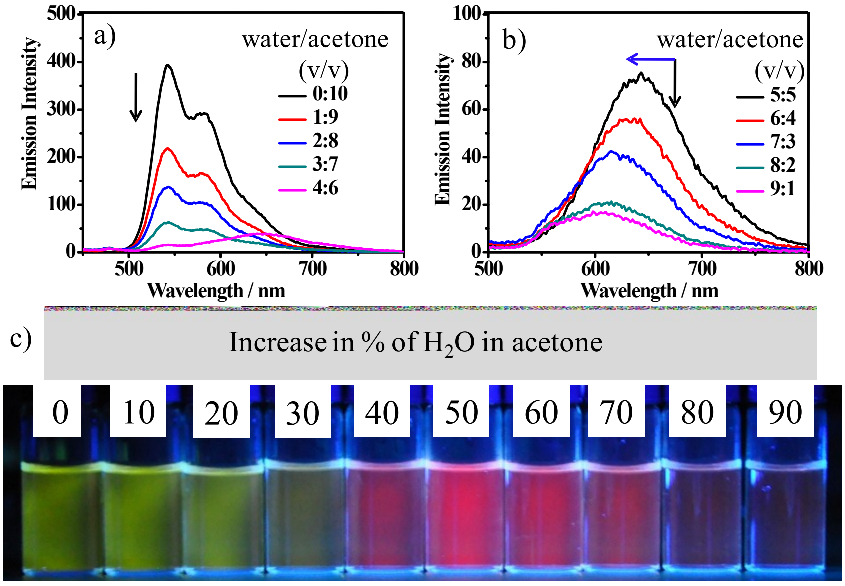

Figure S5. Emission spectra (λ_{ex} = 420 nm) of **Y2** (10^{-5} M) upon increasing the water content in acetone a) from 0 to 40% and b) from 50 to 90%. c) Photographs of **Y2** in water/acetone mixtures under a 365 nm UV lamp.

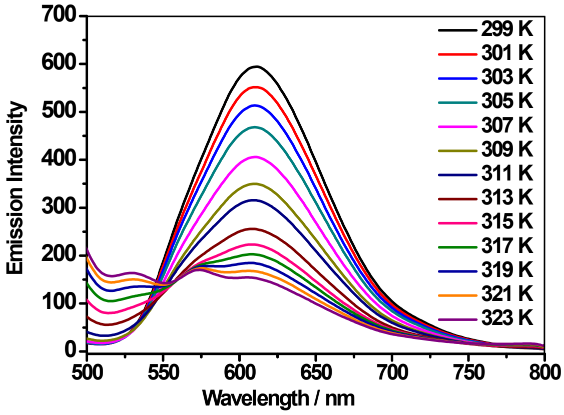

Figure S6. Temperature-dependent emission spectra on heating an aqueous solution of **Y1** (3.2 x 10^{-4} M) from 299 to 323 K.

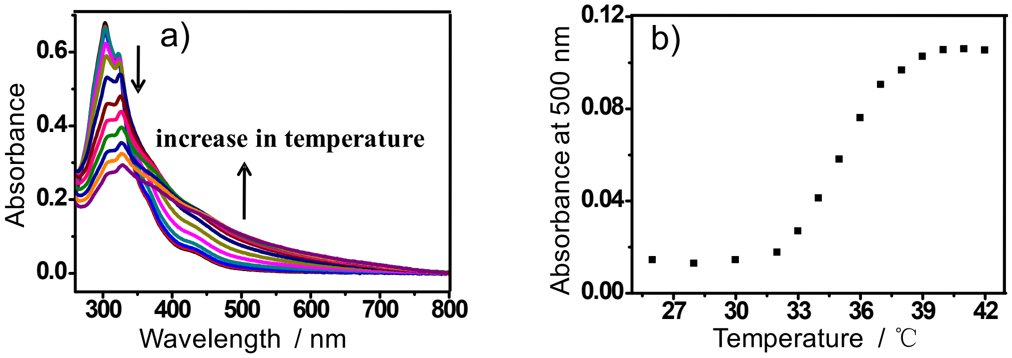

Figure S7. a) Temperature-dependent UV-vis absorption spectra on heating an aqueous solution of **Y2** (5.9×10^{-5} M) from 28 to 42 °C. b) The plots of absorbance against temperature monitored at 500 nm for **Y2**.

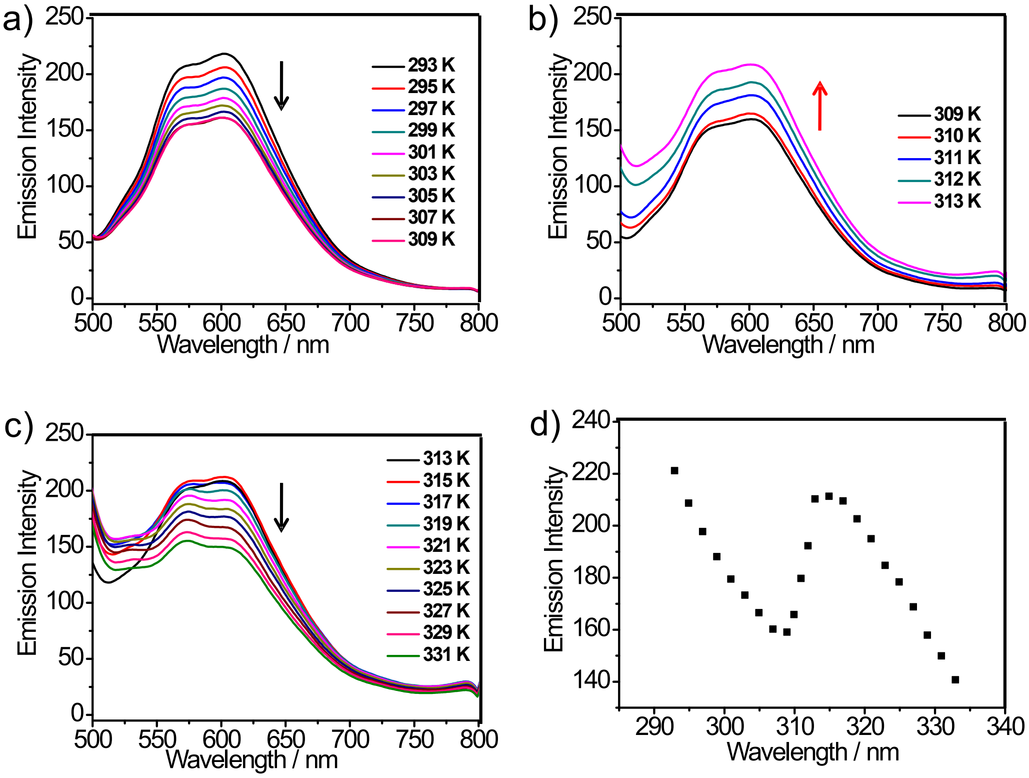

Figure S8. Temperature-dependent emission spectra on heating an aqueous solution of **Y2** (5.9×10^{-5} M) a) from 293 to 309 K; b) from 309 to 313 K and c) from 313 to 331 K. d) The plots of emission intensity against temperature monitored at 600 nm for **Y2**.

4. Tyndall Effect

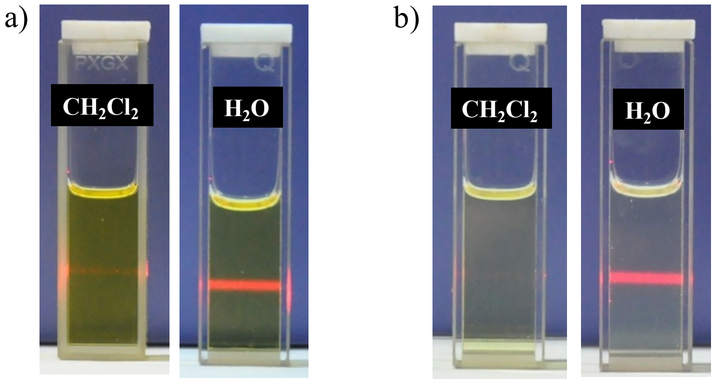

Figure S9. Tyndall effect of a) **Y1** (3.2×10^{-4} M) and b) **Y2** (5.9×10^{-5} M) at different solvents.

5. Multiphase Transition of Metallogel Y2

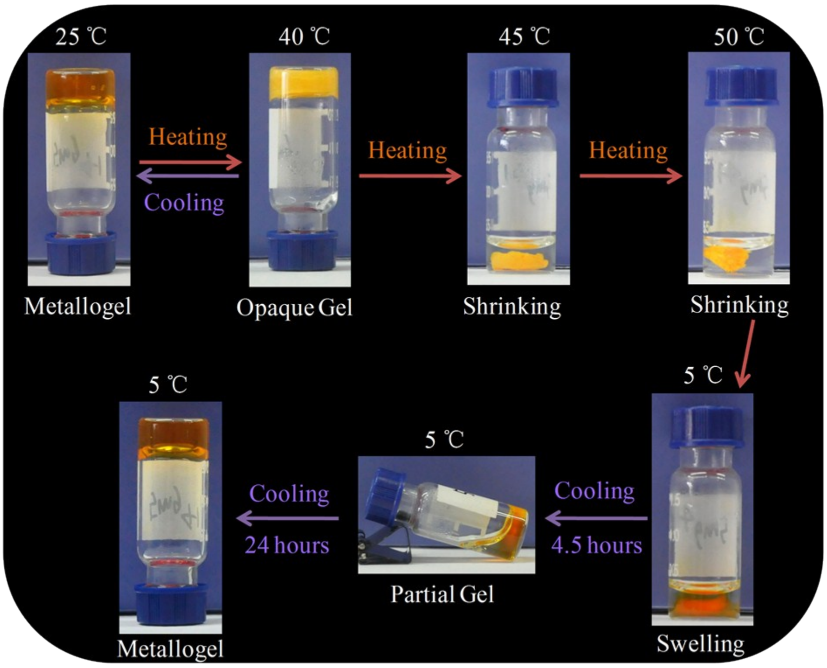

Figure S10. Photographs of the thermally induced phase transition of metallogel **Y2**.

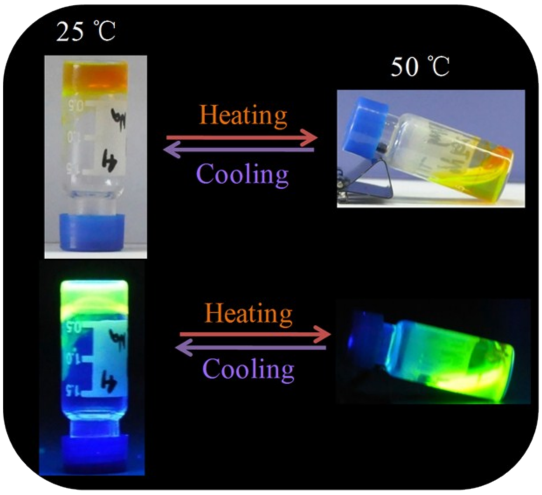

Figure S11. Photographs of the thermally induced reversible encapsulation and release of metallogel **Y2** at ambient light and UV light (365 nm).

6. Determination of T_{cloud} of Compound Y2

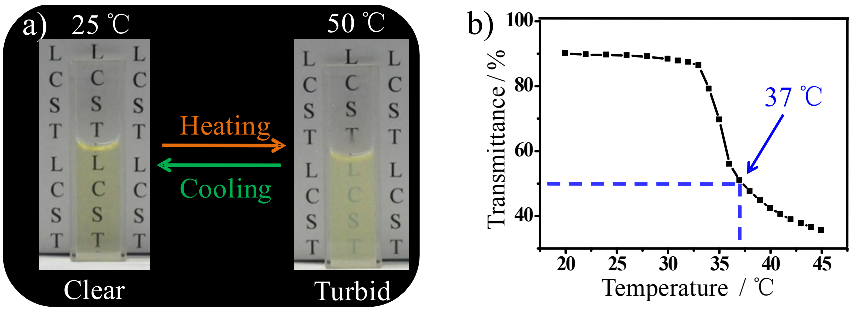

Figure S12. a) Photographs of aqueous solutions of **Y2** below and above LCST. b) Temperature dependence of light transmittance at 506 nm of **Y2** (5.9 x 10^{-5} M) in aqueous solution.

7. Powder X-ray diffraction and concentration-dependent ^{1}H NMR

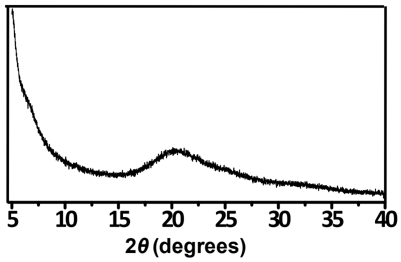

Figure S13. Powder X-ray diffraction pattern of amphiphilic platinum(II) complex **Y2**.

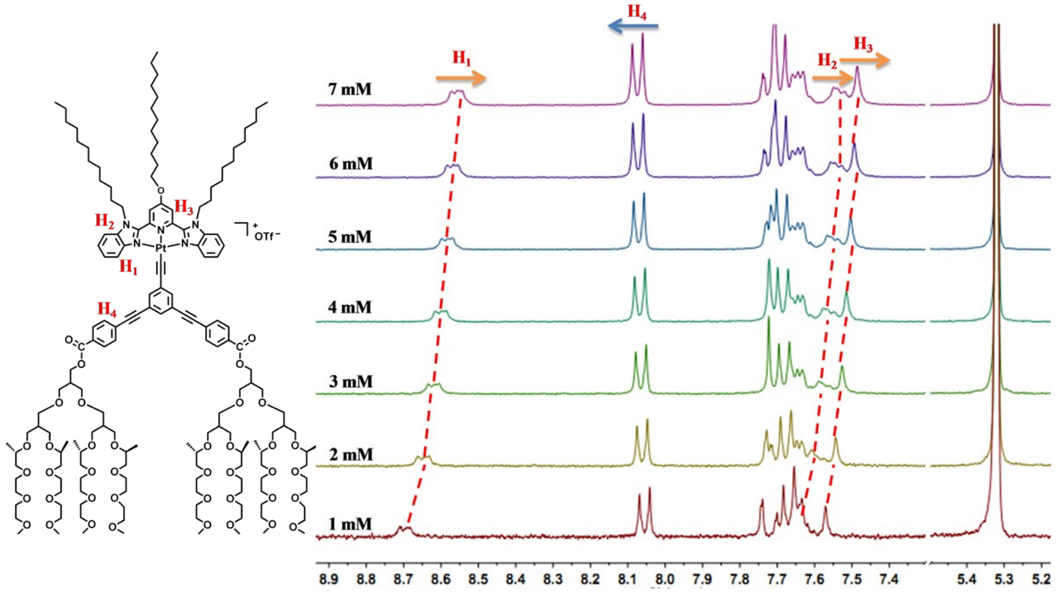

Figure S14. Partial ^{1}H NMR spectra (300 MHz, CD_2Cl_2) of amphiphilic platinum(II) complex **Y2** at different concentrations at 298 K.

8. Rheological characterization

Continuous step strain measurements of both metallogels **Y1** and **Y2** were performed under small (0.1%) and large (5000%) strains, respectively. As shown in Fig. S16b, under the small (0.1%) strain, G’ of metallogel **Y2** was found to be larger than G’’ of metallogel **Y2**, indicating the existence of the free-standing metallogel. However, under the large (5000%) strain, G’’ of metallogel **Y2** was larger than G’ of metallogel **Y2**, instead inferring the conversion from metallogel to sol state. Unexpectedly, the G’ and G’’ of metallogel **Y2** were approximate fully recovered in a half minute even under 5000% strain, and the recovery behavior was repeatable for at least four cycles of different strains. This finding indicated that the resultant metallogel **Y2** might feature a self-healing property. The similar rheological property was also observed for metallogel **Y1** (Fig. S16a).

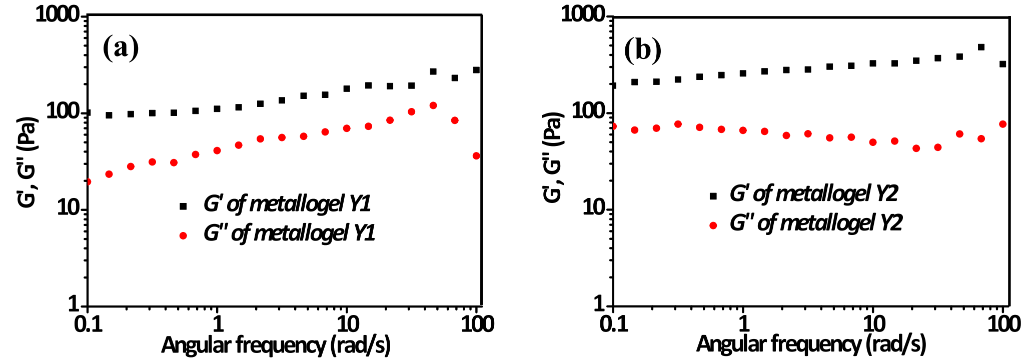

Figure S15. Rheological characterization of (a) metallogel **Y1** and (b) metallogel **Y2**.

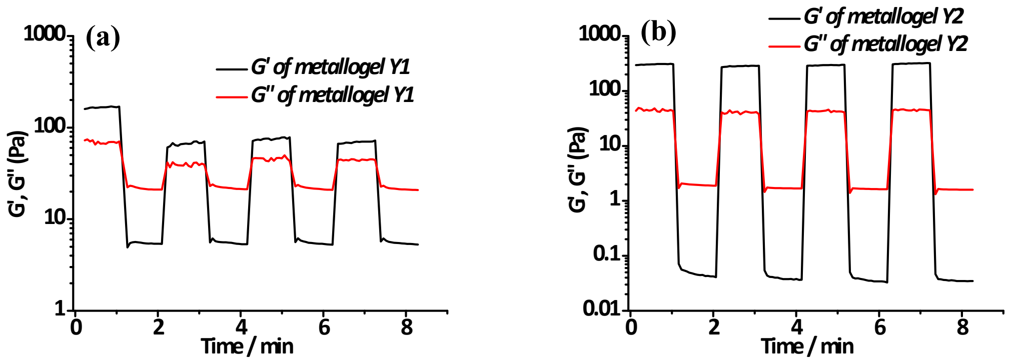

Figure S16. Continuous step strain measurements of (a) metallogel **Y1** and (b) metallogel **Y2**. Metallogels **Y1** and **Y2** were subject to 5000% strain for 30 s, then back to 0.1% strain in the linear regime for 60 s. This process was repeated for four cycles. Measurements were taken at 25 °C with a fixed frequency of 5.0 rad/s.

9. Additional SEM Images

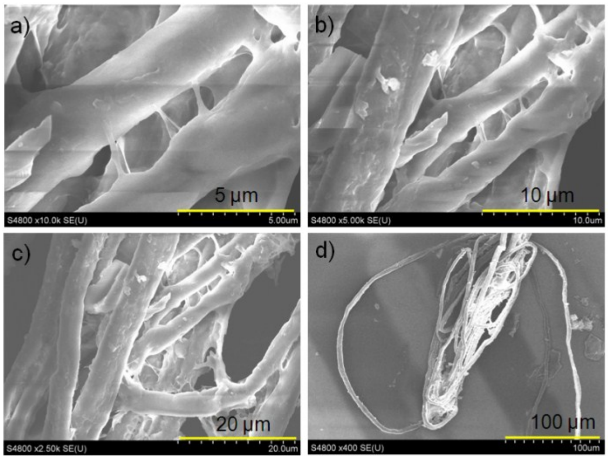

Figure S17. SEM images of Y-shaped amphiphilic complex **Y1** (1.6 x 10^{-4} M) in aqueous solution after increasing the temperature up to 50 ℃ at different scales.

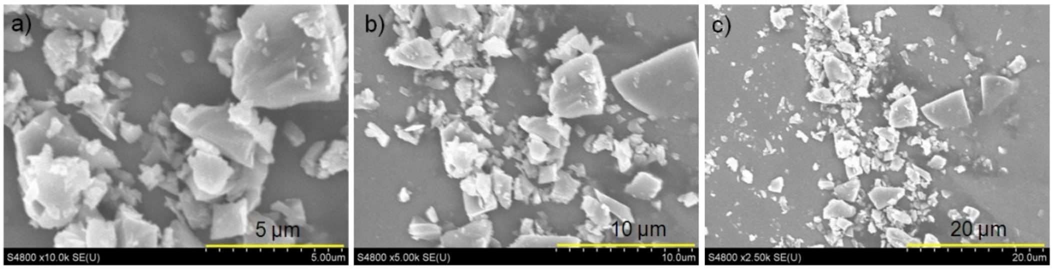

Figure S18. SEM images of Y-shaped amphiphilic complex **Y1** (3.2 x 10^{-4} M) in aqueous solution at 25 ℃ at different scales.

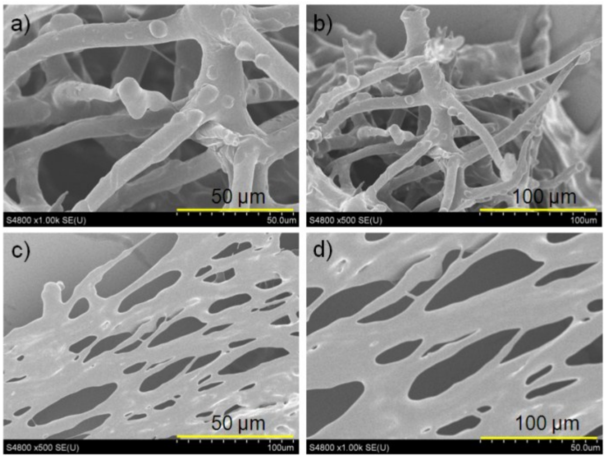

Figure S19. SEM images of Y-shaped amphiphilic complex **Y1** (3.2 x 10^{-4} M) in aqueous solution after increasing the temperature up to 50 ℃ at different scales.

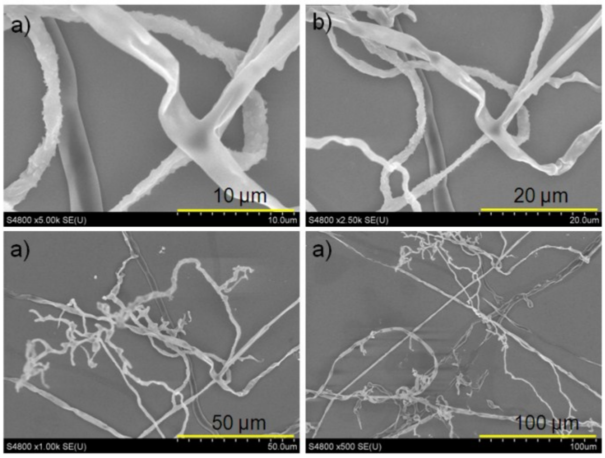

Figure S20. SEM images of the xerogels of Y-shaped amphiphilic complex **Y1** in the mixed solvents of acetone and water (v/v, 1/30) at room temperature.

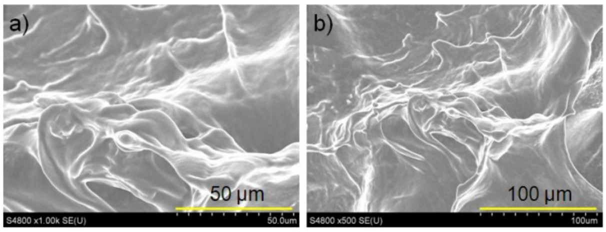

Figure S21. SEM images of metallogel **Y1** in the mixed solvents of acetone and water (v/v, 1/30) after increasing the temperature up to 50 ℃ at different scales.

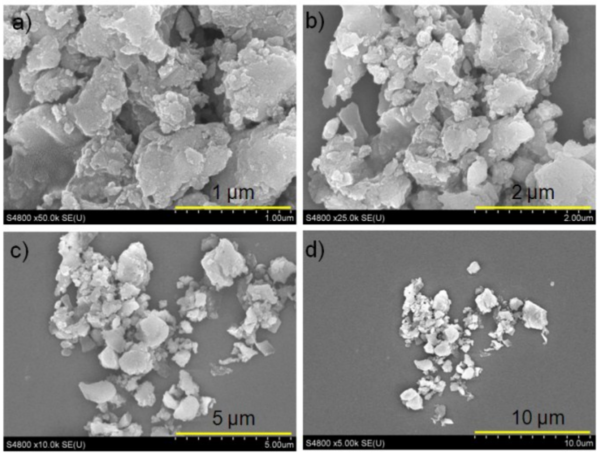

Figure S22. SEM images of Y-shaped amphiphilic complex **Y2** (5.9×10^{-5} M) in aqueous solution at 25 ℃ at different scales.

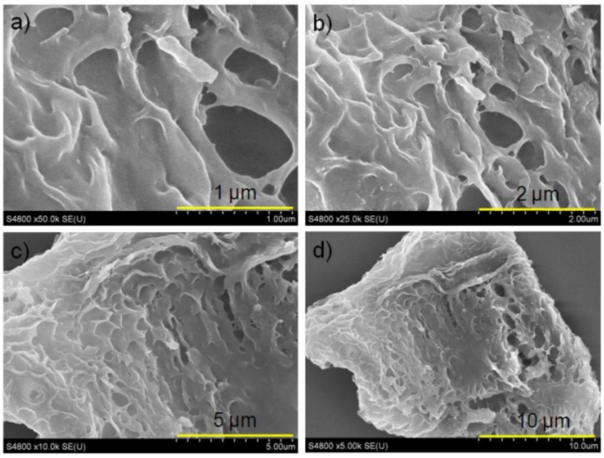

Figure S23. SEM images of Y-shaped amphiphilic complex **Y2** (5.9 x 10^{-5} M) in aqueous solution after increasing the temperature up to 50 ℃ at different scales.

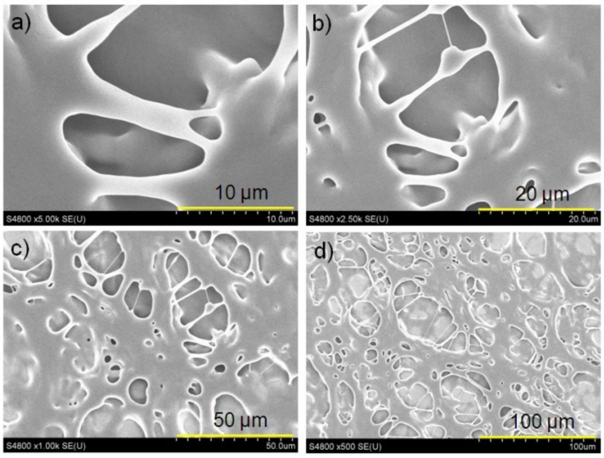

Figure S24. SEM images of the xerogels of Y-shaped amphiphilic complex **Y2** in the mixed solvents of acetone and water (v/v, 1/4) at room temperature.

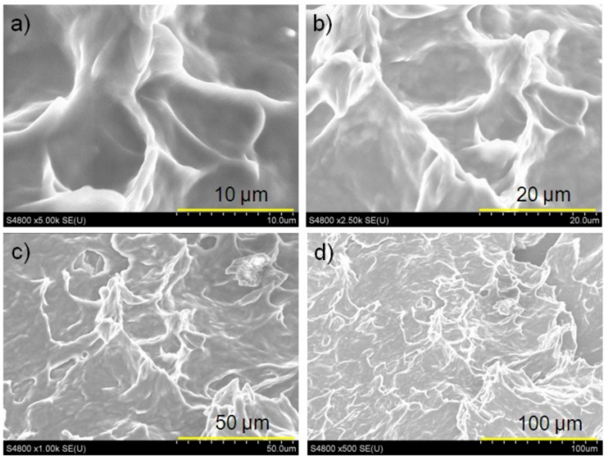

Figure S25. SEM images of metallogel **Y2** in the mixed solvents of acetone and water (v/v, 1/4) after increasing the temperature up to 50 ℃ at different scales.

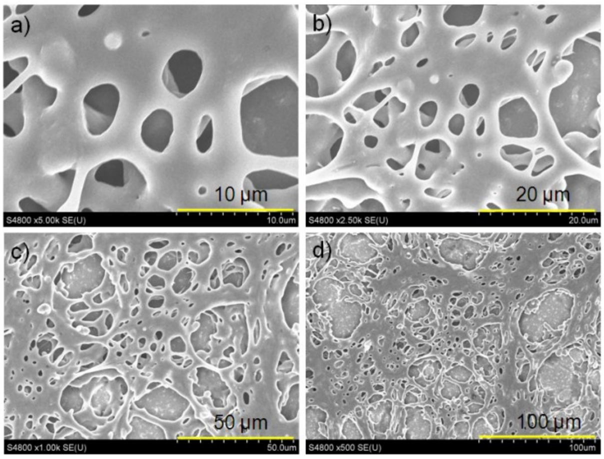

Figure S26. SEM images of metallogel **Y2** after the addition of fluorescein sodium at room temperature.

10. Multiple Nuclear NMR (^{1}H and ^{13}CNMR) Spectra and MALDI-TOF MS of New Complexes

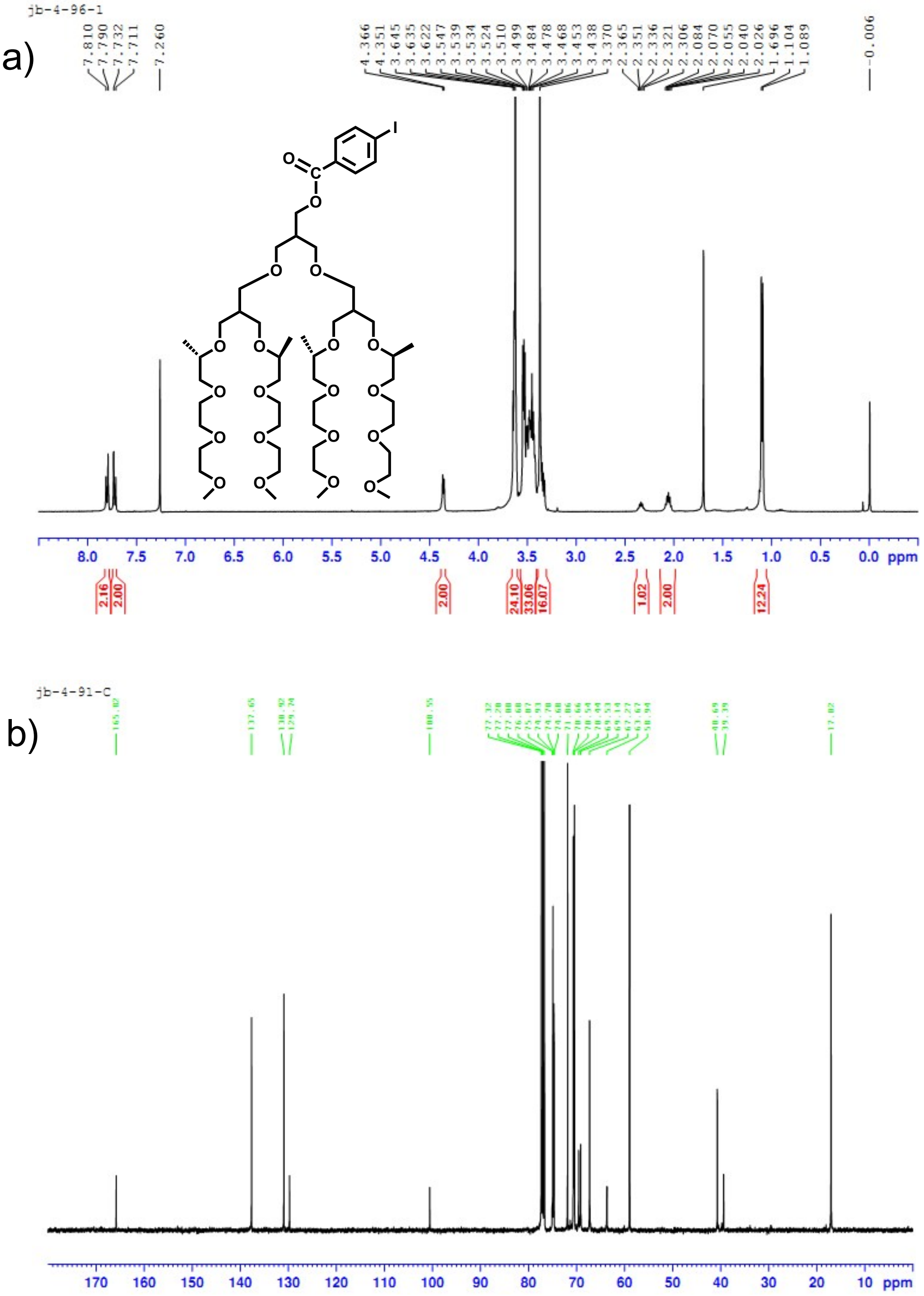

Figure S27. a) ^{1}H NMR and b) ^{13}C NMR spectra of compound **3** in $CDCl_3$.

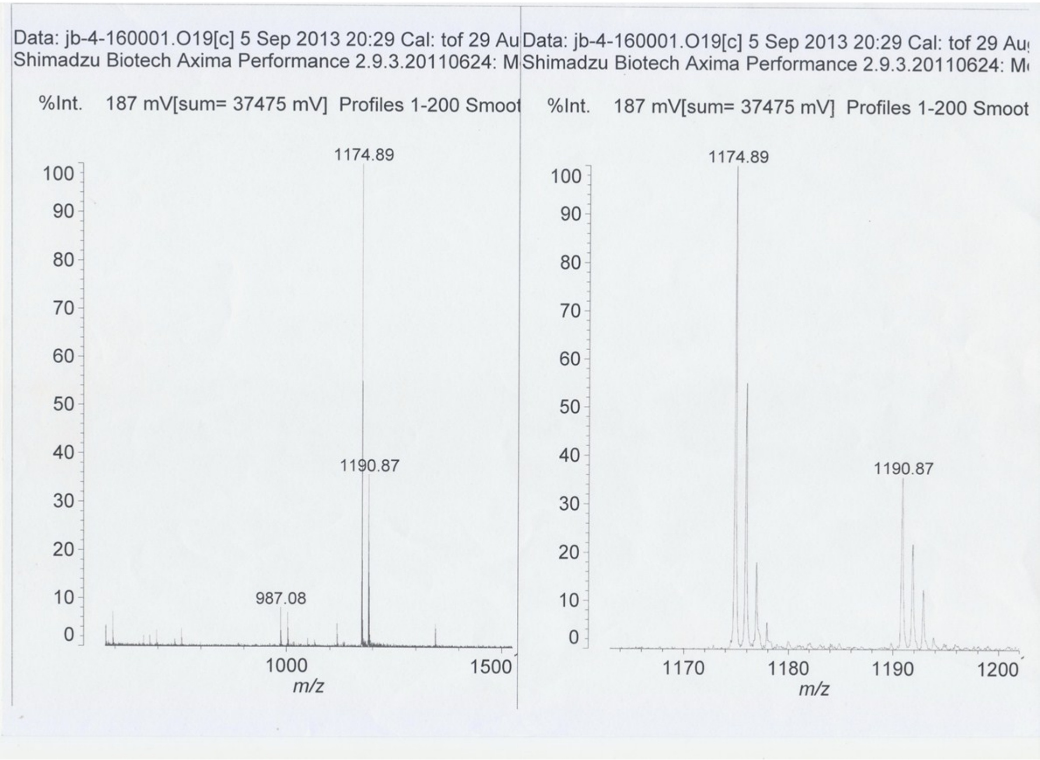

Figure S28. MALDI-TOF-MS of **3**: m/z calcd for $C_{51}H_{93}INaO_{20}$ ($[M+Na]^+$): 1175.52, found: 1174.89.

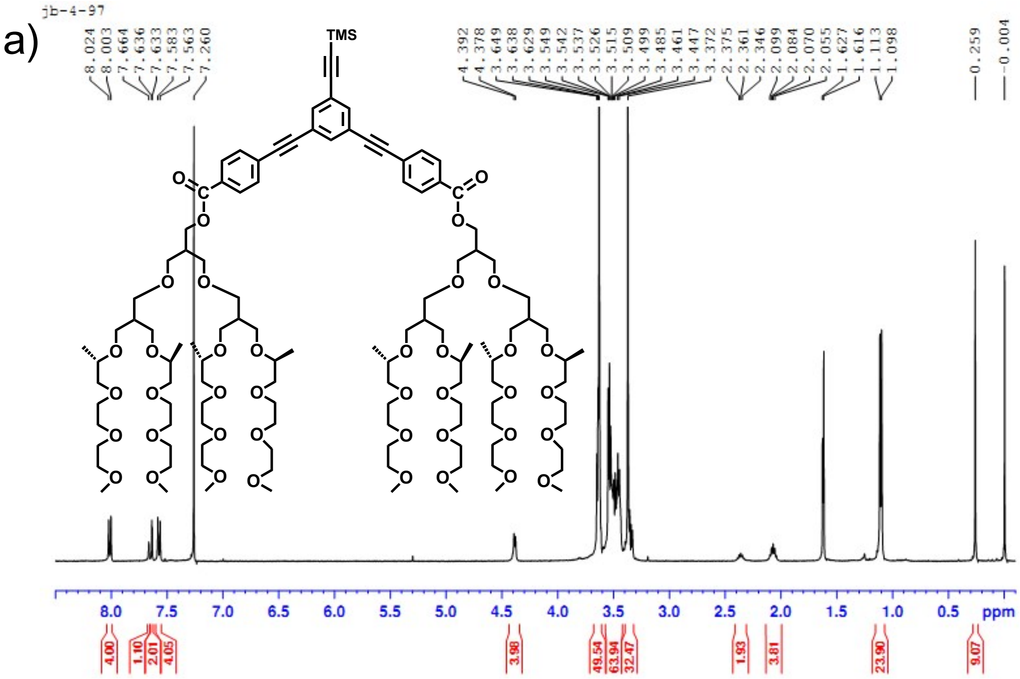

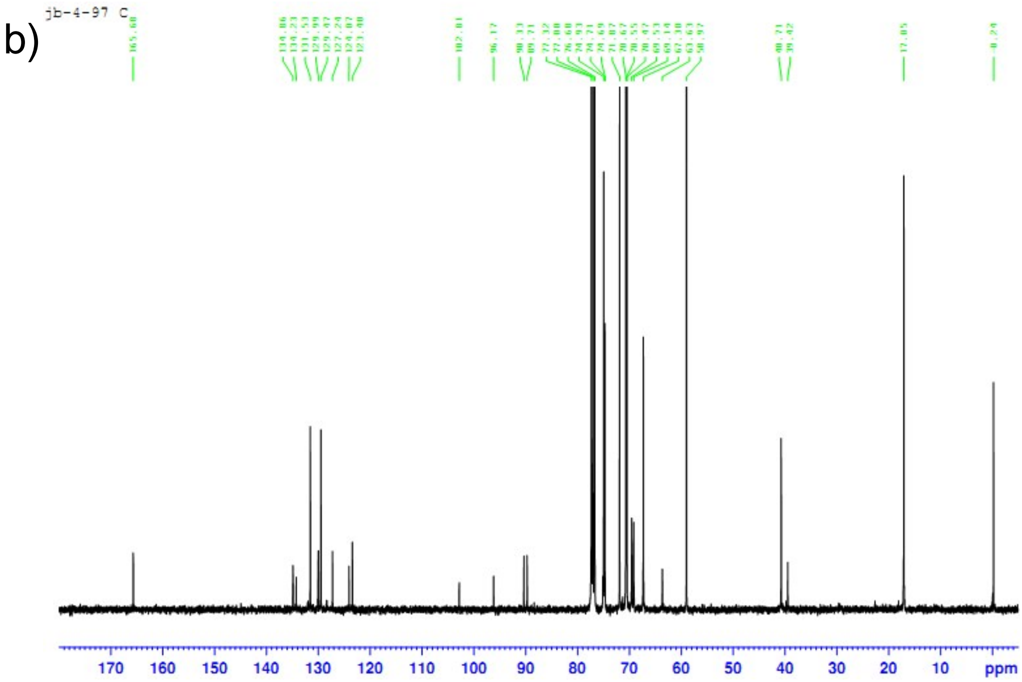

Figure S29. a) ^{1}H NMR and b) ^{13}C NMR spectra of compound **5** in $CDCl_3$.

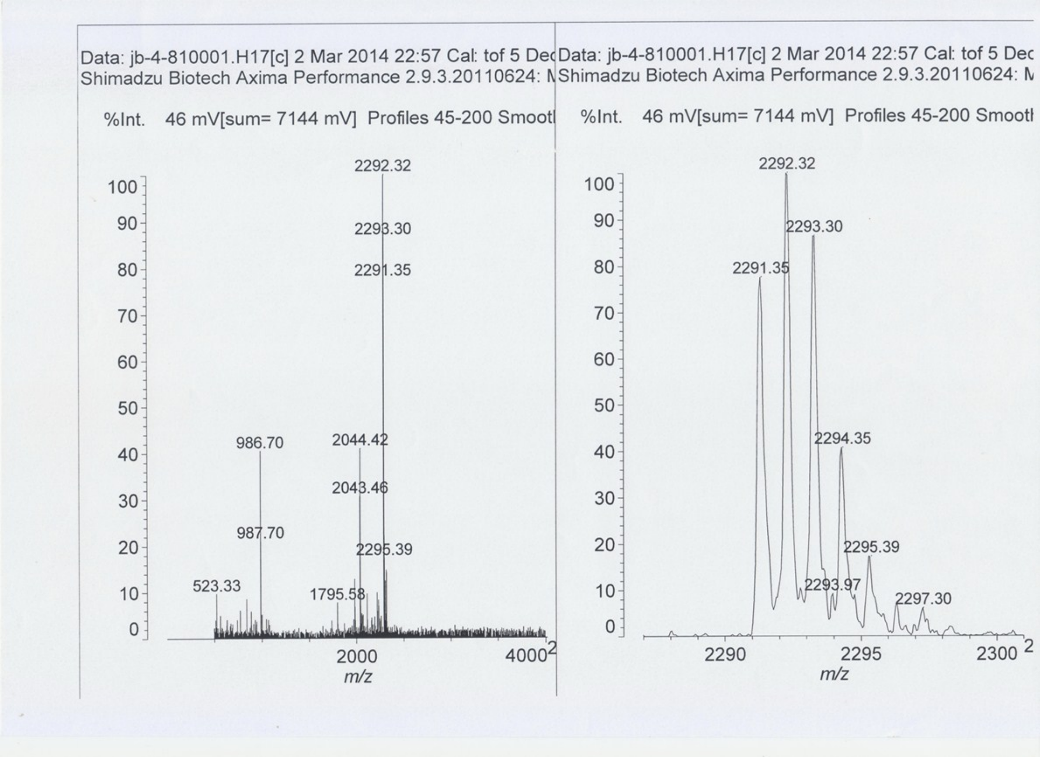

Figure S30. MALDI-TOF-MS of **5**: m/z calcd for $C_{117}H_{198}NaO_{40}Si$ ($[M+Na]^+$): 2294.31, found: 2292.32.

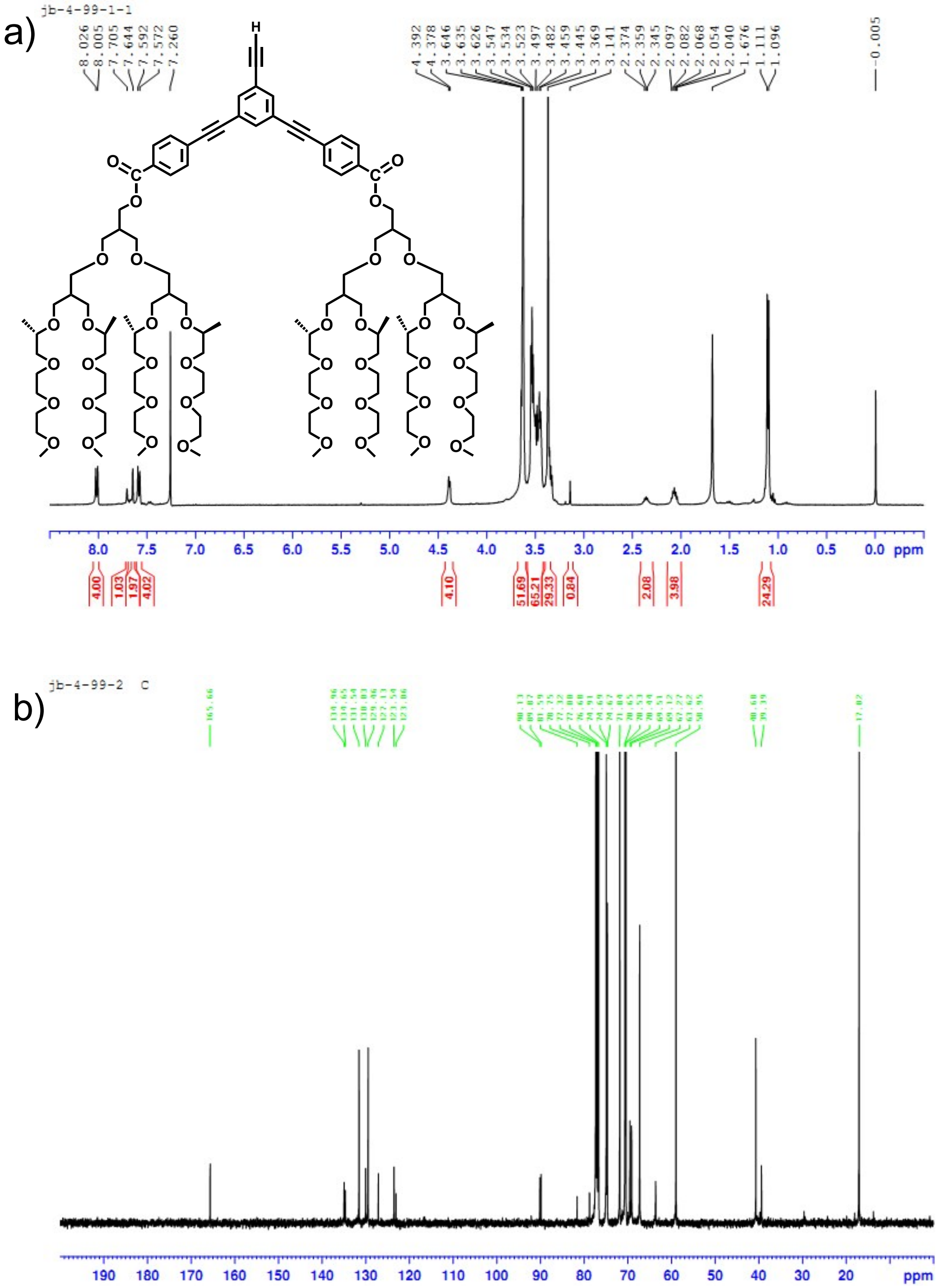

Figure S31. a) ^{1}H NMR and b) ^{13}C NMR spectra of compound **6** in $CDCl_3$.

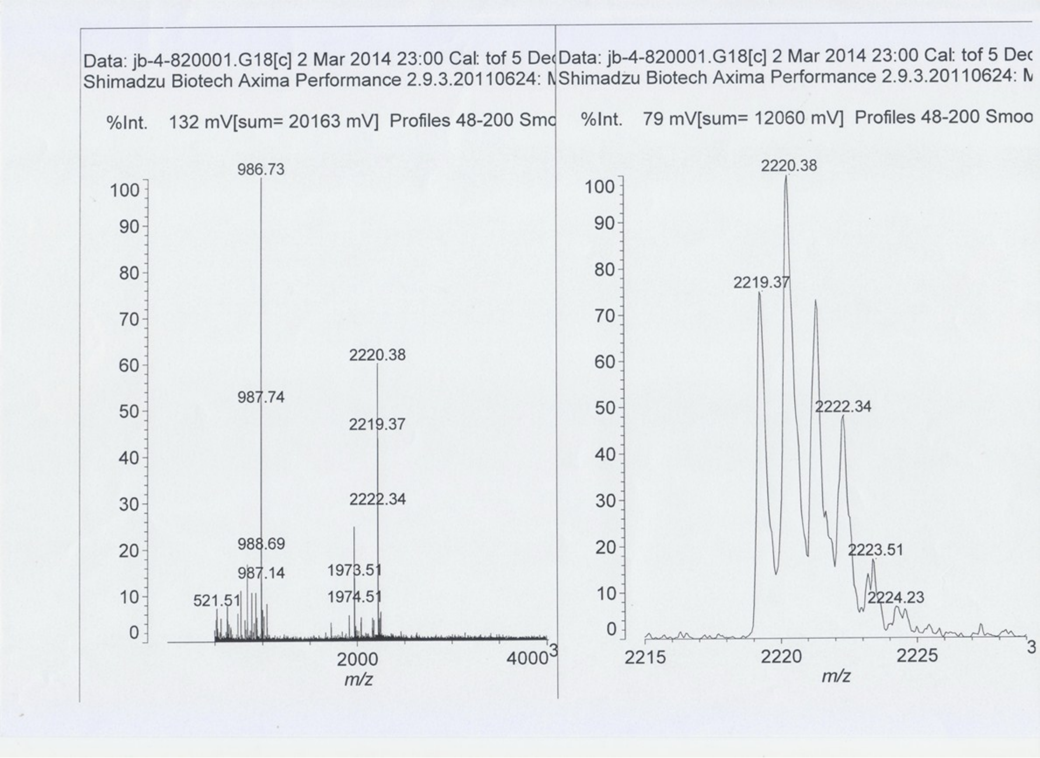

Figure S32. MALDI-TOF-MS of **6**: m/z calcd for $C_{114}H_{190}NaO_{40}$ ($[M+Na]^+$): 2222.27, found: 2220.38.

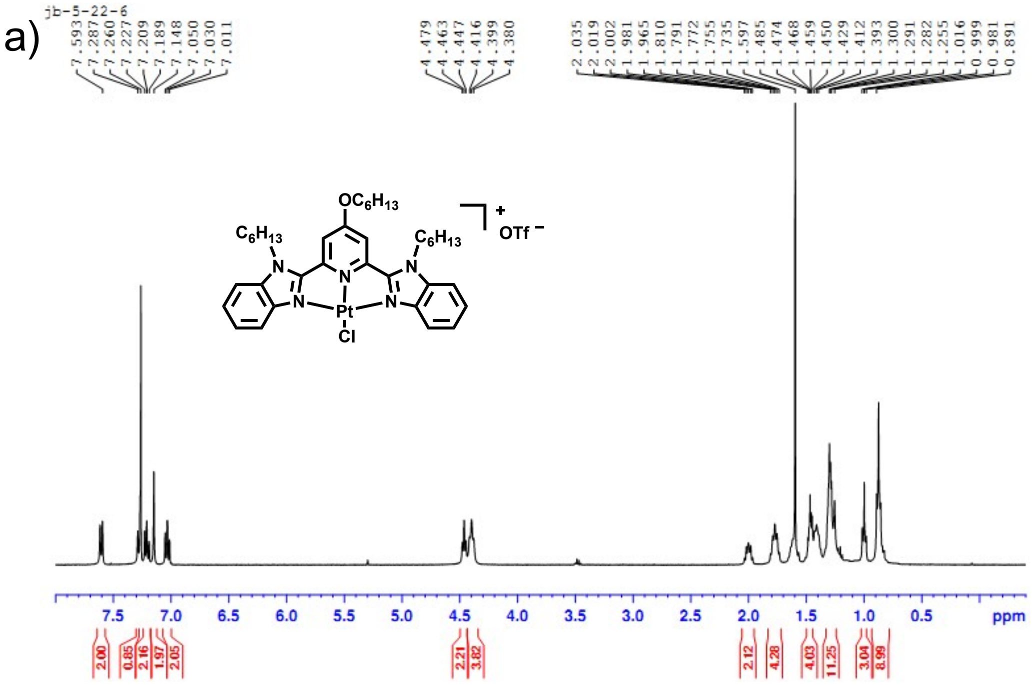

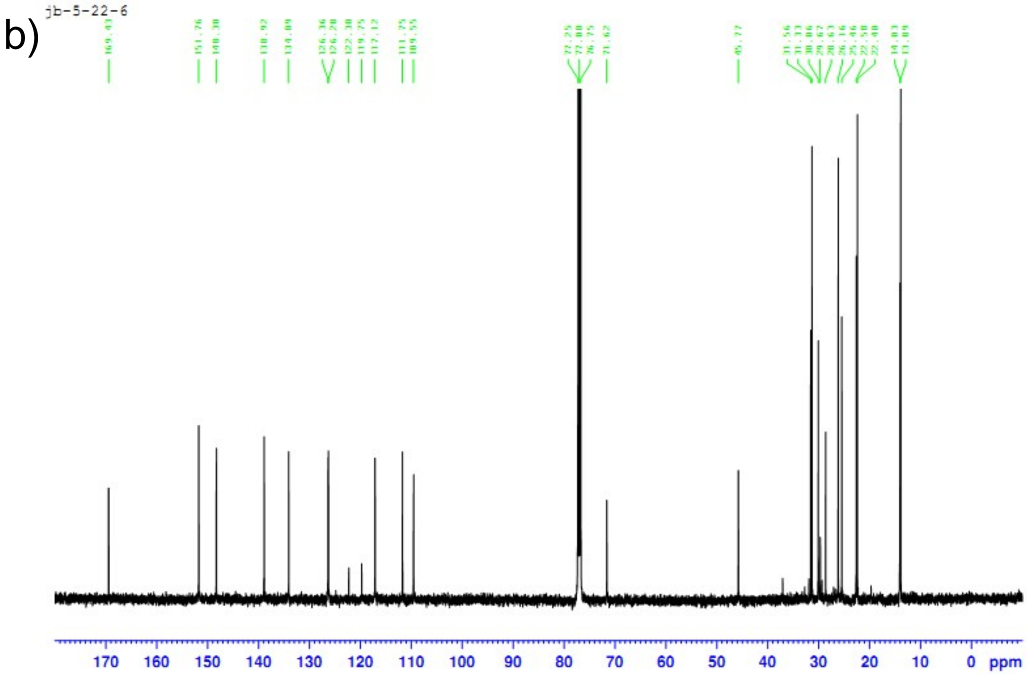

Figure S33. a) ^{1}H NMR and b) ^{13}C NMR spectra of compound **7** in $CDCl_3$.

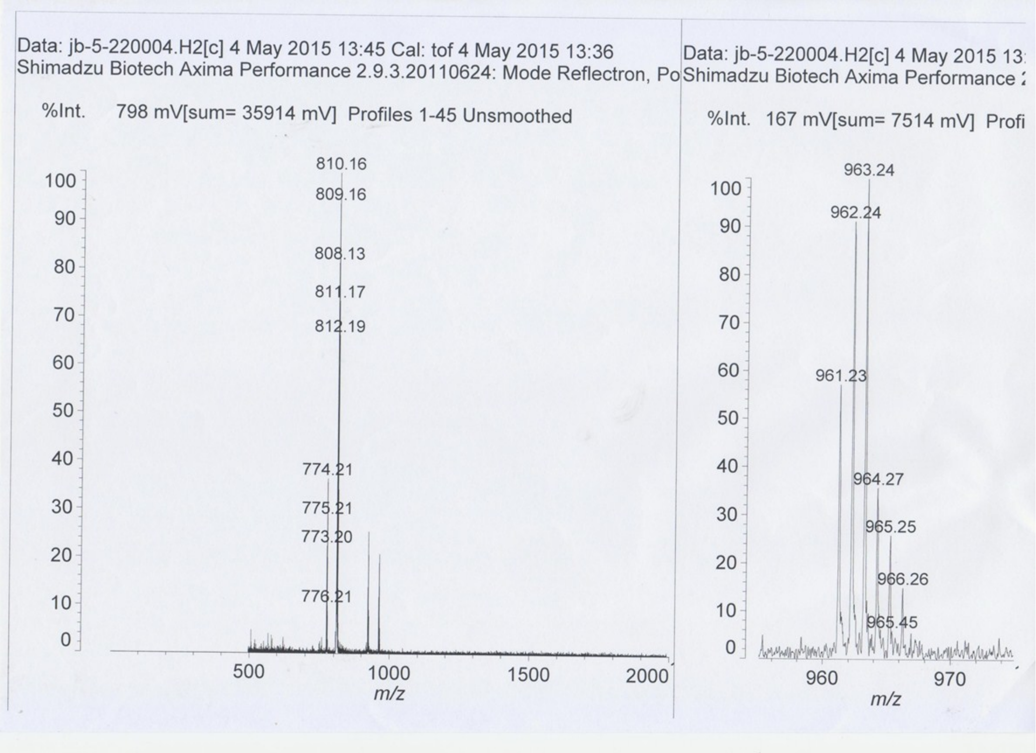

Data: jb-5-220004.H2[c] 4 May 2015 13:45 Cal: tof 4 May 2015 13:36
Shimadzu Biotech Axima Performance 2.9.3.20110624: Mode Reflectron, Po
%Int. 798 mV[sum= 35914 mV] Profiles 1-45 Unsmoothed

Data: jb-5-220004.H2[c] 4 May 2015 13:
Shimadzu Biotech Axima Performance 2
%Int. 167 mV[sum= 7514 mV] Profi

Figure S34. MALDI-TOF-MS of **7**: m/z calcd for $C_{37}H_{49}ClN_5OPt$ ($[M-OTf]^+$): 809.33, found: 810.16.

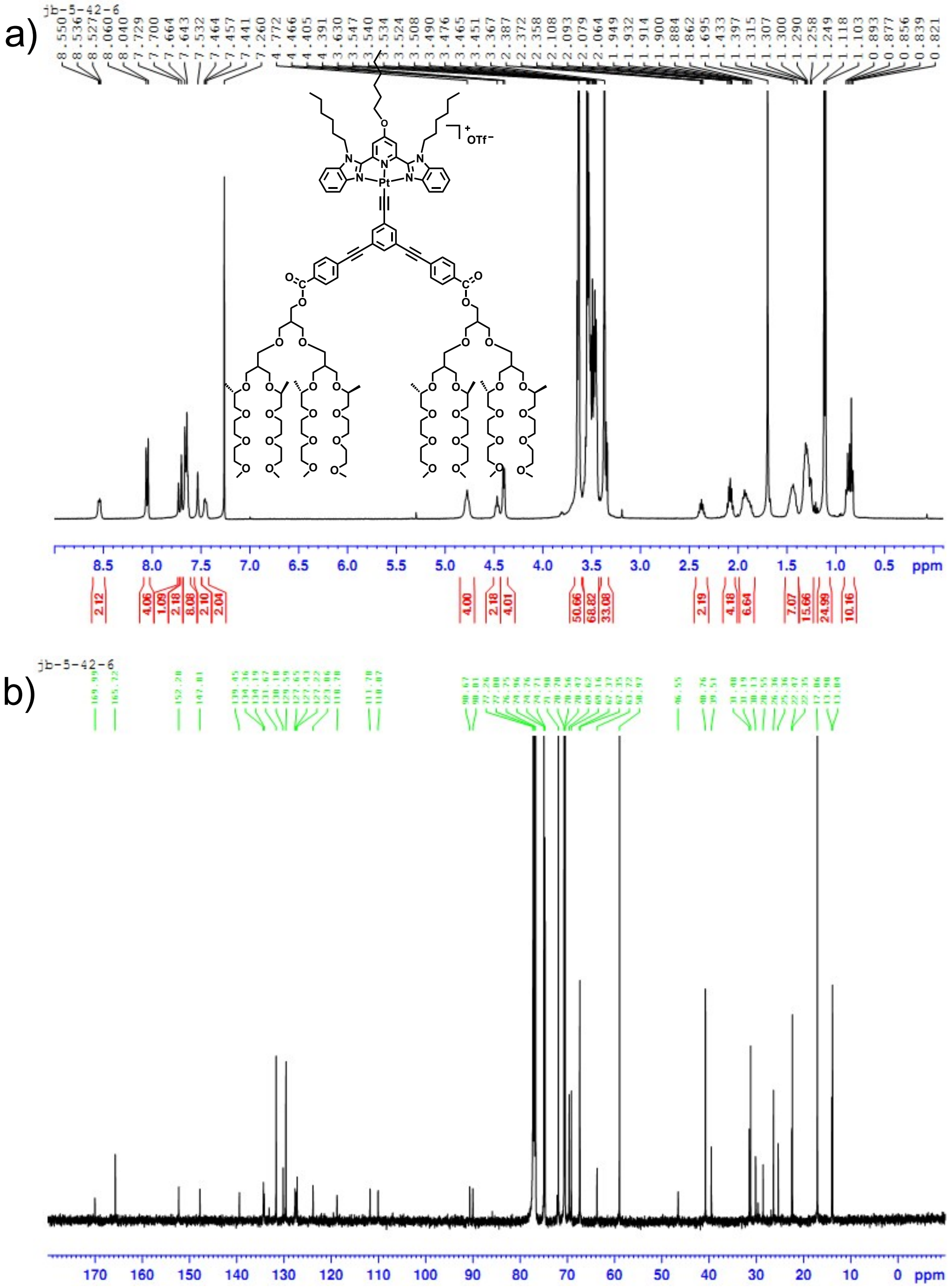

Figure S35. a) ^{1}H NMR and b) ^{13}C NMR spectra of Y-shaped amphiphilic alkynylplatinum(II) bzimpy complex **Y1** in $CDCl_3$.

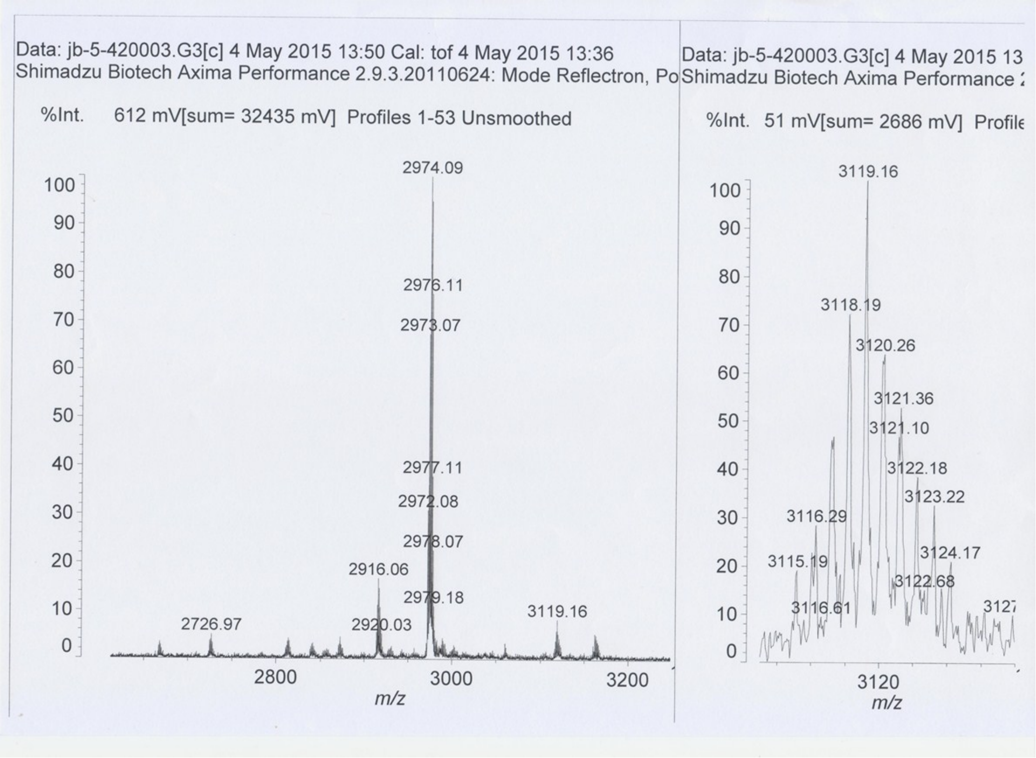

Figure S36. MALDI-TOF-MS of **Y1**: m/z calcd for $C_{151}H_{238}N_5O_{41}Pt$ ($[M\text{-}OTf]^+$): 2972.63, found: 2974.09.

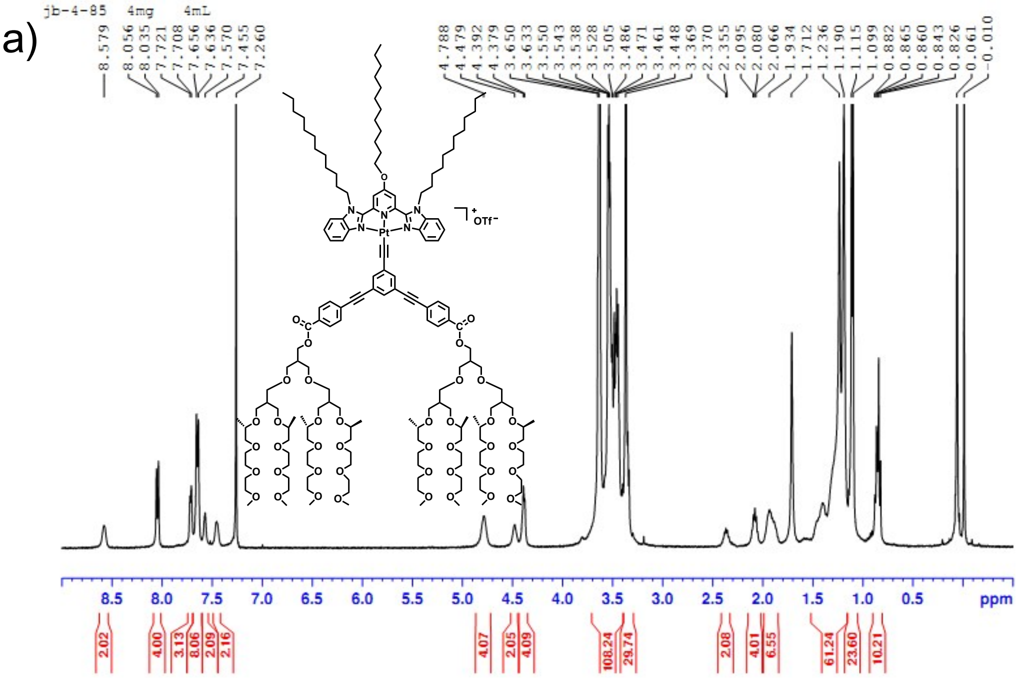

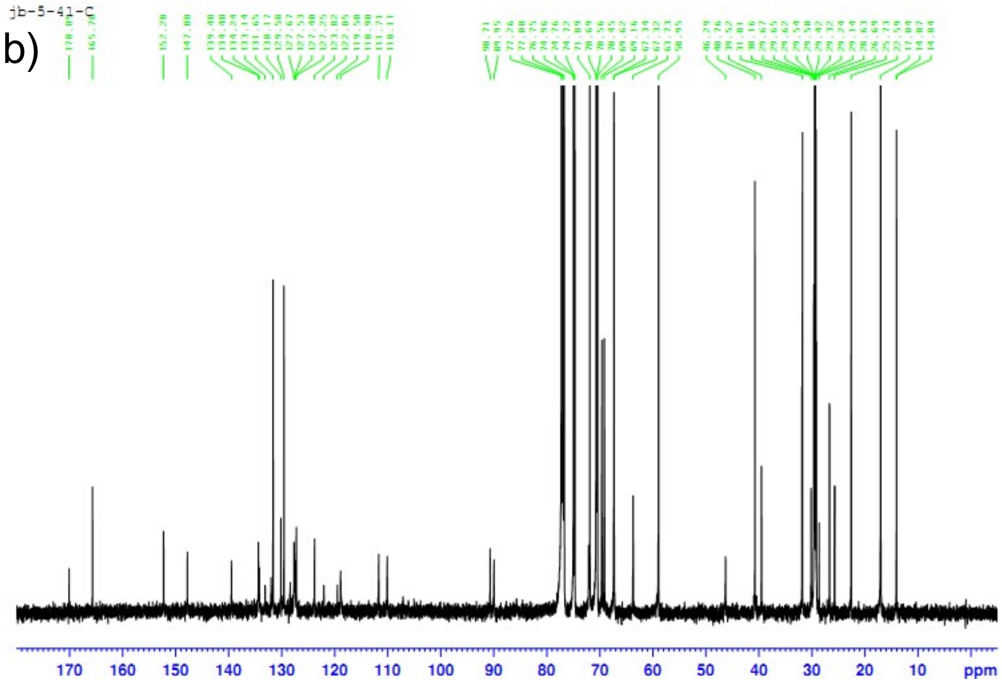

Figure S37. a) ^{1}H NMR and b) ^{13}C NMR spectra of Y-shaped amphiphilic alkynylplatinum(II) bzimpy complex **Y2** in $CDCl_3$.

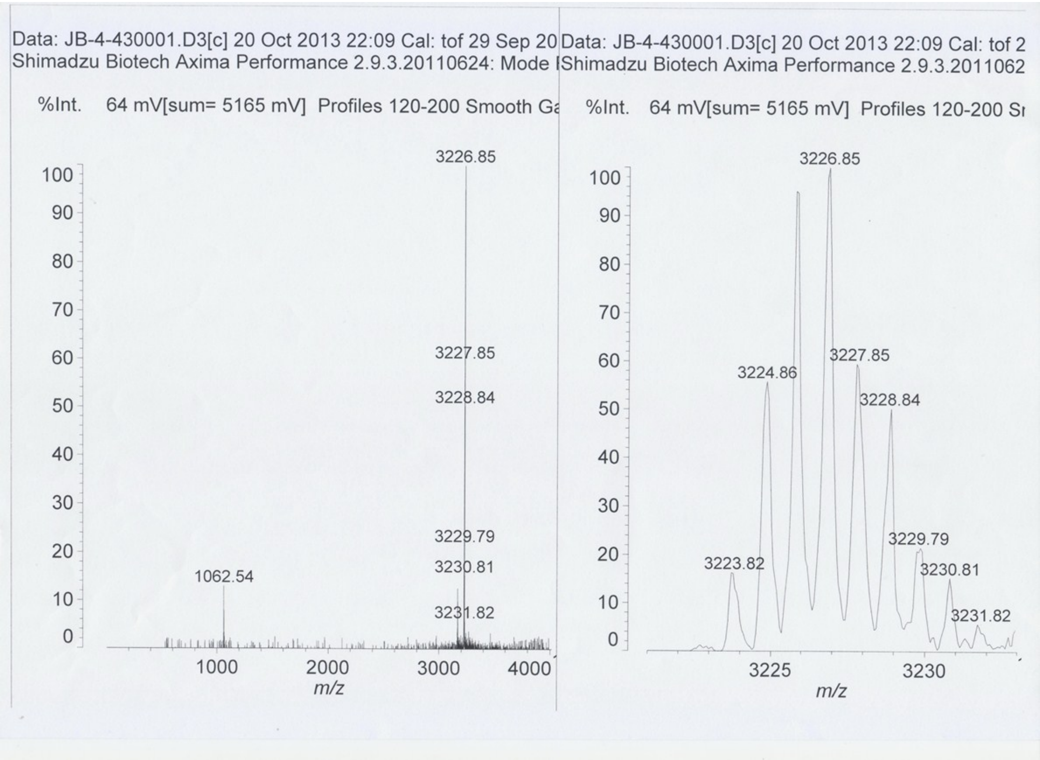

Figure S38. MALDI-TOF-MS of **Y2**: m/z calcd for $C_{169}H_{274}N_5O_{41}Pt$ ($[M-OTf]^+$): 3224.92, found: 3226.85.